Supporting Information

Swaggart et al. 10.1073/pnas.1324242111

SI Materials and Methods

Detailed Breeding Scheme. Sixteen (male = 8, female = 8) F_1 heterozygous $Sgcg^{D2/129}$ animals were generated from five F_0 breeding pairs. All F_0 sires were DBA/2J (D2) and heterozygous ($^{+/-}$) or null ($^{-/-}$) for *Sgcg*. All dams were 129T2/SvEmsJ (129) and WT, heterozygous, or null for *Sgcg*. Heterozygous *Sgcg* status of F_1 animals was determined by PCR using the following primers: GGAGGAAGCGCTGCCTATACCTATT, CAAATGCTTGCCTCAGGTATTTC, and GCCTGCTCTTTACTGAAGGCTCTTT. F_2-null $Sgcg^{D2/129}$ animals were generated from nine breeding pairs comprised of heterozygous $Sgcg^{D2/129}$ animals. Homozygous null *Sgcg* status of F_2 animals was determined by PCR; 189 (male = 96, female = 93) F_3-null $Sgcg^{D2/129}$ animals were generated from 22 unique breeding pairs comprised of null $Sgcg^{D2/129}$ animals. An average of 8.59 F_3 animals were generated from each breeding pair, with a minimum of 3 animals and a maximum of 16 animals per breeding pair. PCR was used to confirm homozygous null status of F_3 animals.

WT 129T2/SVEmsJ (129) and WT C57BL/6J mice were bred for one generation to generate mice that were heterozygous for the severe allele at the *Anxa6* locus called $WT^{129/B6}$. *Sgcd* mice were previously described (1).

RT-PCR. RNA was isolated from the abdominal muscle and the ventricles of the hearts of WT^{D2}, WT^{129}, $Sgcg^{D2}$, and $Sgcg^{D2}$ animals. Approximately 30 mg of tissue was disrupted using a mortar and pestle or electric homogenizer. RNA extraction was performed using the RNeasy Mini Kit (Qiagen) with on-column DNase digestion following manufacturer guidelines. cDNA was synthesized using qScript cDNA SuperMix (Quanta Biosciences) following manufacturer guidelines. Control reactions were performed with RNA processed using the same method but without RT. PCR was performed for *Anxa6* exons 4/5 to exon 15 and exons 9/10 to exon 15 using the following primers: Anxa6_4.5F: ATGGCAAGGACCTCATCGAAGACT, Anxa6_9.10F: ACAGCACCTACGACTGGTGTTTGA, Anxa6_15R: CAATTCCCTTCATGGCTTTCCGCA. These reactions detect the full-length and alternate *Anxa6* transcripts with expect product sizes of 927 and 580 and 515 and 168 bp, respectively. To specifically detect the alternate transcript, the following primer was used: Anxa6_11.15.16R, CAGTTCCAATTCCCTTCATGGCTTTCCGCAAAAT. Using the exon 4/5 and exon 9/10 forward primers, the expected product sizes for these reactions are 174 and 580 bp, respectively. For all reactions, 35 cycles were performed with annealing at 63 °C for 30 s and extension at 72 °C for 1 min. Sanger sequencing was performed following treatment of PCR products with ExoSAP-IT (Affymetrix) following manufacturer guidelines to determine the identity of the alternate transcript.

Immunoblotting. Abdominal muscle and the ventricles of the heart from WT^{D2}, WT^{129}, $Sgcg^{D2}$, and $Sgcg^{D2}$ animals were harvested and homogenized in whole tissue lysis buffer [50 mM Hepes, pH 7.5, 150 mM NaCl, 2 mM EDTA, 10 mM NaF, 10 mM Na-pyrophosphate, 10% (vol/vol) glycerol, and 1% Triton X-100] with half of a Complete, Mini protease inhibitor mixture pill (Roche). Protein concentration was determined by the BioRad Protein assay, and 100 μg of protein was run overnight on 12% SDS-polyacrylamide gels. Transfer was performed without SDS to Immobilon-P PVDF membranes (Millipore). Transferred protein was visualized with MemCode Reversible Protein Stain (Pierce) following manufacturer instructions and used as a loading control. Membranes were blocked in 6% instant nonfat dry milk in Tris-buffered saline with 0.1% Tween 20 (TBS-T) for 1 h at room temperature. Following blocking, membranes were incubated with an N-terminal rabbit polyclonal anti-ANXA6 IgG antibody (ab31026; Abcam) at 1:250 in block for 1 h at room temperature. The membranes were washed with TBS-T. The membranes were then incubated with goat anti-rabbit IgG HRP-conjugated antibody (Novex) at 1:7,500 in block for 1 h at room temperature. Following wash, blots was developed with Amersham ECL Prime (GE Healthcare), imaged using the UVP Biospectrum Imaging System (UVP) and manipulated in Adobe Photoshop CS4.

Plasmids. The alternate *Anxa6* ORF was subcloned from B6 heart RNA using the following primers: HindIII_Anxa6_F AAGCTTATGGCCAAAATAGCACAGGGTGCCATG, Anxa6_7.8_ApaI_R GGGCCCCGTCATTCTCCCGGGTTCCCTGGAGC, Anxa6_4.5F ATGGCAAGGACCTCATCGAAGACT and Alt3-prime_AmpR GGGCCCCTCGAGGTTCCAATTCCCTTCATGGCTTTCCGCAAAATACTCCGGGGTGCTTCGGATGCACTTCACCACGG. The full alternate *Anxa6* ORF was cloned into a modified pcDNA3 vector using HindIII and XhoI (New England Biolabs). The full-length *Anxa6*-GFP clone was purchased from Origene (MG222645). A carboxyl-terminal EGFP tag was inserted into ANXA6N32 using BamH1 and Xho1 restriction enzymes.

Anxa6 rs26961431 Genotyping. The region of the *rs26961431* variant was amplified from DNA of the 163 animals used in the quantitative trait locus (QTL) analysis using the following primers: Anxa6_11seqAF GGAGCAAGTTAGTGAGTTAACCTGGTTG and Anxa6_11seqAR GCAGCAGGATTCGCCATGATCTCTG. Thirty cycles were performed with annealing at 65 °C for 30 s and extension at 72 °C for 1 min with an expected product size of 507 bp. After treatment with ExoSAP-IT following manufacturer instructions, samples were Sanger sequenced. Analysis was performed in Prism 4.0 (GraphPad) using one-way ANOVA and Tukey's multiple comparison test. Graphs are presented with mean and 95% CI.

Immunofluorescence Microscopy. Muscles were harvested from Evans blue dye-injected $Sgcg^{D2}$, $Sgcg^{129}$, $Sgcd^{D2}$, and $Sgcd^{129}$ animals and flash frozen in liquid nitrogen. Ten-micrometer sections were cut, fixed in 4% paraformaldehyde for 10 min at room temperature, and then washed in PBS on ice for 30 min. Sections were blocked in 10% BSA with 0.1% Triton at 4 °C for 1 h. Sections were incubated in block containing anti-annexin A6 amino-terminal antibody (Abcam ab31026) at 1:100 overnight at 4 °C and then washed in PBS on ice for 30 min. Secondary Alexa Fluor 488-conjugated antibody was incubated 1:2,500 at 4 °C for 1 h. Slides were then washed and mounted with Vectashield (Vector Laboratories). D2 and 129 images were collected identically using an Axioskop microscope (Carl Zeiss) and iVision software (BioVision Technologies) or on a Leica SP5 2 photon microscope with LAS AF Leica Imaging Software and manipulated for brightness/contrast/color in Adobe Photoshop.

Dysferlin staining was with anti-dysferlin (1:100; NCL Hamlet). Donkey anti-rabbit Alexa 488 and donkey anti-mouse Alexa 350 secondary antibodies were used at 1:2,500. Slides were mounted in Vectashield and imaged identically on a Leica SP5 2 photon microscope. Images were processed identically in Image J.

ANXA6N32-GFP Expression Analysis. The mean fluorescent intensity of GFP was measured from time 0 (prelaser damage) in ANXA6N32-GFP electroporated fibers using Image J. Fibers

were binned into low or high expressing fibers based on the mean fluorescent intensity of GFP. FM4-64 internalization was plotted as F/F_0 between the low and high expressing groups. Statistics were performed using Prism 4.0 (Graphpad).

1. Hack AA, et al. (2000) Differential requirement for individual sarcoglycans and dystrophin in the assembly and function of the dystrophin-glycoprotein complex. *J Cell Sci* 113(Pt 14):2535–2544.

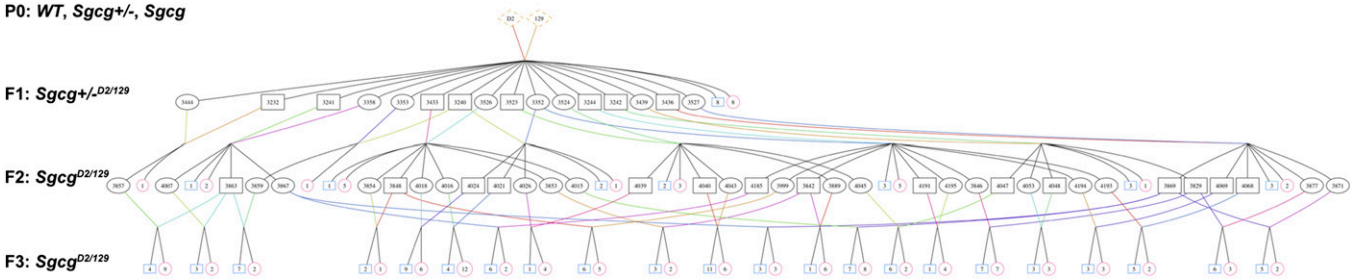

Fig. S1. A genetically diverse F_3 $Sgcg^{D2/129}$ cohort was used for QTL mapping. Animals used for mapping were generated through an intercross of *DBA/2J* (D2) and *129T2/SvEmsJ* (129) animals. *Sgcg* null, heterozygous, and WT P0 animals were used to create an F_1 cohort of *Sgcg* heterozygous animals on a mixed D2/129 background. Heterozygous F_1 animals were bred to create a cohort of F_2 *Sgcg*-null animals on a mixed D2/129 background. These F_2 *Sgcg*-null animals were interbred to generate the F_3 $Sgcg^{D2/129}$ cohort. Shown is the pedigree of the F_3 animals used in this study. Orange diamonds represent male or female P0 animals. Black squares represent breeding males, black circles represent breeding females; numbers are animal IDs. Blue squares and pink circles indicate the number of male and female progeny, respectively, from each breeding pair. Black lines indicate sibling relationships. Colored lines represent breeding relationships.

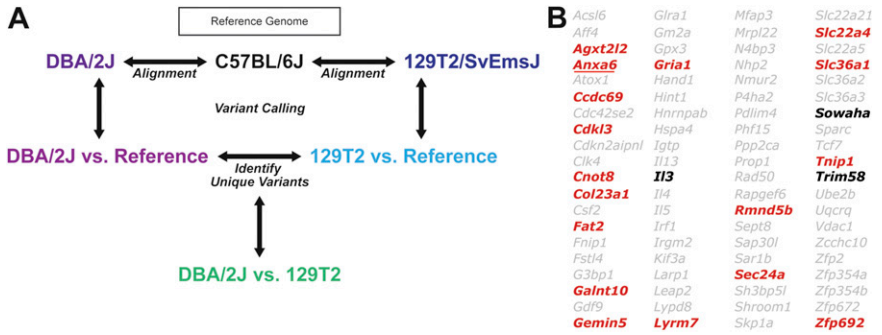

Fig. S2. Whole genome and RNA sequencing to identify *Anxa6* in the chromosome 11 QTL interval. (*A*) To identify genetic variation between the parental strains used for QTL mapping, whole genome sequencing and variant analysis were performed. The 129T2/SvEmsJ (129, blue) genome was sequenced to more than 50-fold coverage, aligned to the mouse reference genome C57BL/6J (B6), and variants were called between the two genomes. The DBA/2J (D2) genome was from the Wellcome Trust Sanger Institute Mouse Genomes Project (www.sanger.ac.uk/sanger/Mouse_SnpViewer/rel-1303). The D2 vs. B6 and 129 vs. B6 variant calls were then compared with identify variants that distinguish the D2 and 129 genomes from one another. (*B*) Named protein coding genes (excluding olfactory receptors) within the smallest overlapping chromosome 11 interval are shown. Genes in red are expressed in the heart as detected by RNA sequencing and also contained coding variation. Genes in black indicate that the gene contains coding variation. *Anxa6* encoding annexin A6 was the most highly expressed sequence that contained genic variation.

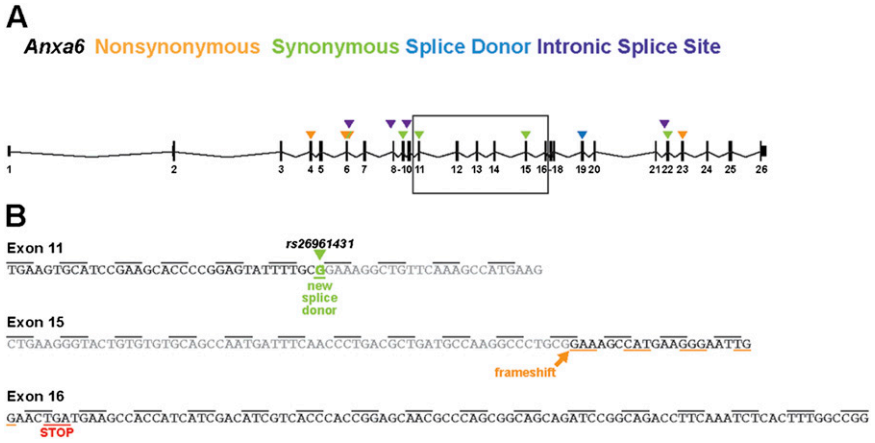

Fig. S3. Variation in the *Anxa6* gene. (*A*) Variants detected are shown across the *Anxa6* gene. (*B*) A G/A change creates a splice donor in *Anxa6* in the DBA2/J and C57Bl6/J strains. The position of the G/A is also known as *rs26961431*, which was used for genotyping. The *Anxa6′* splice variant joins exon 11 with exon 15, resulting in a frameshift and premature stop codon in exon 16.

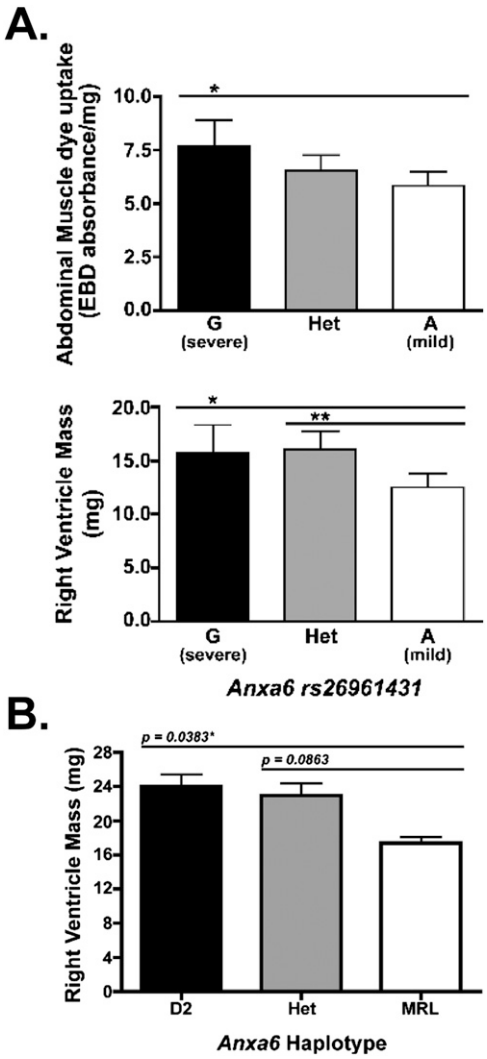

Fig. S4. *rs26961431* correlates significantly with muscle membrane leak and right ventricle mass. The variant in exon 11 of *Anxa6* was previously identified as *rs26961431* and encodes a G/A SNP between the DBA/2J (D2) and 129T2/SvEmsJ (129) inbred mouse strains. (*A*) Evans blue dye (EBD) uptake in the abdominal muscle group was significantly different based on *rs26961431* genotype ($P = 0.0168$, ANOVA). Animals with the *G* allele (severe) have significantly more dye uptake than animals with the *A* allele (mild) ($*P < 0.05$, Tukey posttest). Right ventricle mass was significantly different based on *rs26961431* genotype ($P = 0.0013$, ANOVA). Animals homozygous for the severe *G* allele found in D2 or heterozygous at *rs26961431* had significantly larger right ventricles than animals homozygous for the mild *A* allele found in the 129 strain ($*P < 0.05$ and $**P < 0.01$, respectively, Tukey posttest). (*B*) The *Anxa6* region of chromosome 11 was also associated with right ventricular mass in *Sgcg* mice from an MRL X 129 cross generated with same method as previously described (1).

1. Heydemann A, et al. (2012) The superhealing MRL background improves muscular dystrophy. *Skelet Muscle* 2(1):26.

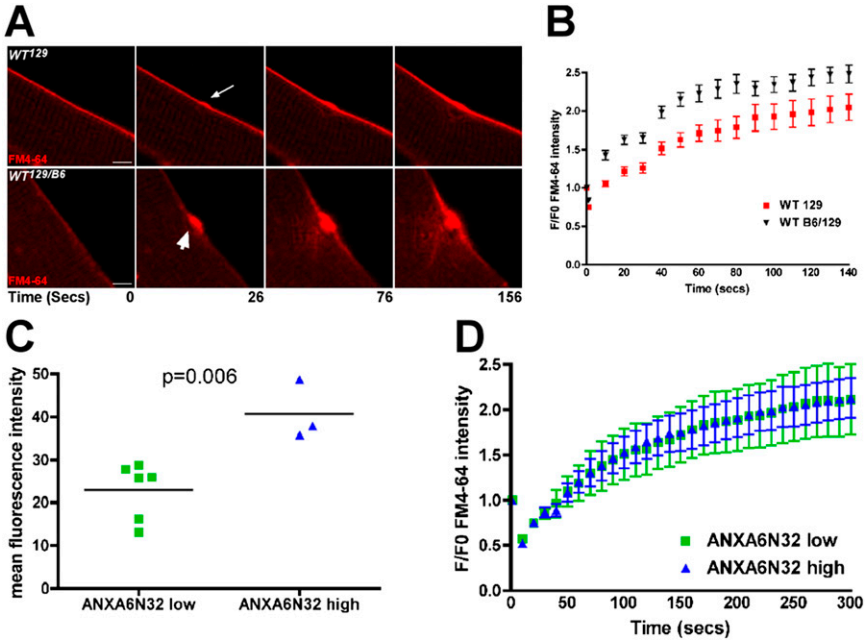

Fig. S5. ANXA6N32 impairs sarcolemmal repair. (*A*) Fibers from 129/B6 intercrossed mice displayed reduced repair compared with those from the 129 background. FM4-64 fluorescence is shown at times after laser damage. (*B*) The results were quantified using the F/F0 ratio demonstrating that heterozygous B6/129 fibers have slower repair compared with those from the 129 background, indicating that low levels of ANXA6N32 disrupt sarcolemmal repair. (*C*) Electroporated fibers were scored for low and high expression of ANXA6N32 based on mean fluorescence intensity. (*D*) Fibers with both low and high expression of ANXA6N32 had equivalent delay in resealing as measured by the F/F0 ratio.

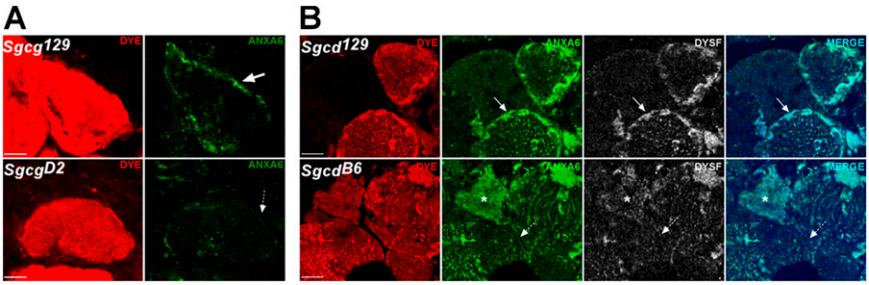

Fig. S6. Reduced membrane associated annexin A6 in EBD-positive myofibers from the D2 and B6 strains. (*A*) Confocal imaging of EBD-positive fibers, which have disrupted sarcolemma. Compare arrows in top images to dashed arrow in lower image. There was less membrane associated annexin A6 in dye positive fibers from the D2 background. (*B*) Muscles from mice lacking δ-sarcoglycan, *Sgcd* mice, which are a model of LGMD 2F (1), showed a similar pattern as *Sgcg* mice. *Sgcd* mice on the 129 background showed more sarcolemmal associated annexin A6 immunoreactivity compared with those on the B6 background, which also contains SNPs encoding ANXAN32 (compare arrow in *Upper* compared with dashed arrow in *Lower*). Some dye-positive fibers contained internalized annexin A6 (asterisk), and these same fibers also contained internalized dysferlin staining (see merged image).

1. Hack AA, et al. (2000) Differential requirement for individual sarcoglycans and dystrophin in the assembly and function of the dystrophin-glycoprotein complex. *J Cell Sci* 113(Pt 14): 2535–2544.

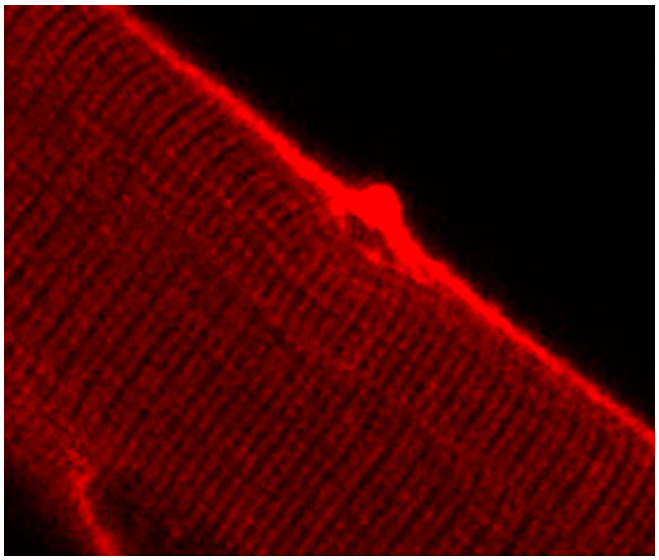

Movie S1. Mild muscle damage in WT^{129} myofibers. Laser induced damage was used in the presence of FM4-64 to asses sarcolemmal injury and repair. A representative time lapse movie of a WT^{129} myofiber is shown. FM4-64 slowly and minimally enters the myofiber at the site of laser damage. The 129 strain harbors the mild *Anxa6* allele.

Movie S1

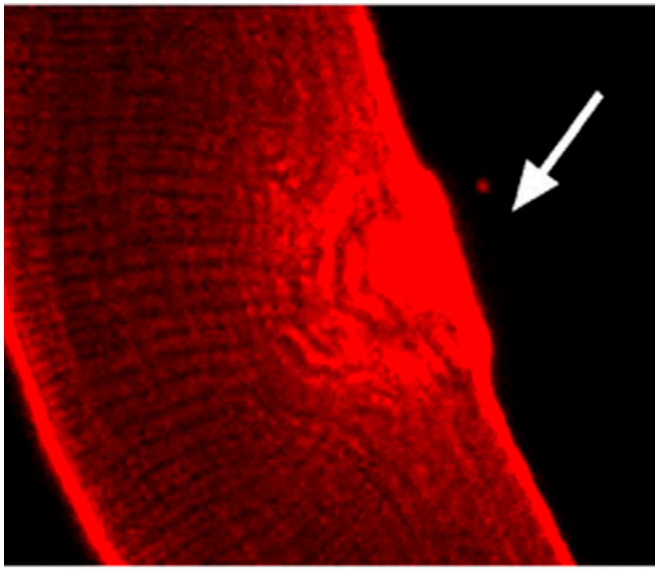

Movie S2. Severe muscle damage in WT^{D2} myofibers. Laser induced damage was used in the presence of FM4-64 to asses sarcolemmal injury and repair. A representative time lapse movie of a WT^{D2} myofiber is shown. FM4-64 quickly and continuously enters the myofiber at the site of laser damage. FM4-64 leaks from the site of damage. The D2 background harbors the severe allele of *Anxa6*.

Movie S2

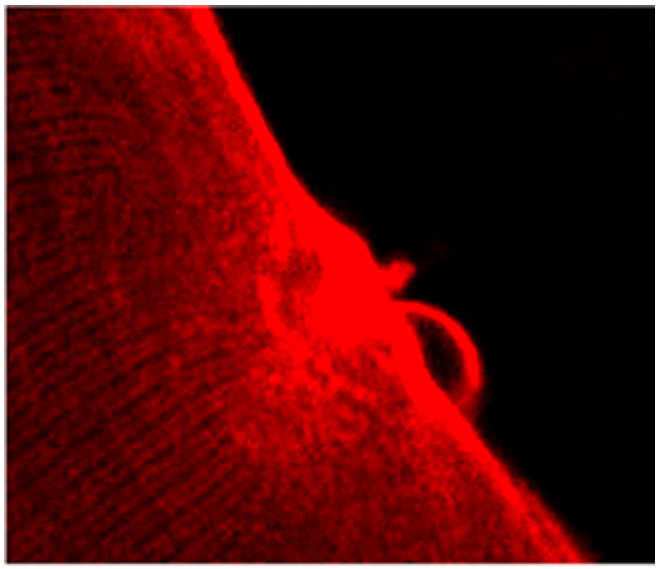

Movie S3. Severe muscle damage in WT^{B6} myofibers. Laser induced damage was used in the presence of FM4-64 to asses sarcolemmal injury and repair. A representative time lapse movie of a WT^{B6} myofiber is shown. FM4-64 quickly and continuously enters the myofiber at the site of laser damage. FM4-64 leaks from the site of damage. The B6 background harbors the severe allele of *Anxa6*.

Movie S3

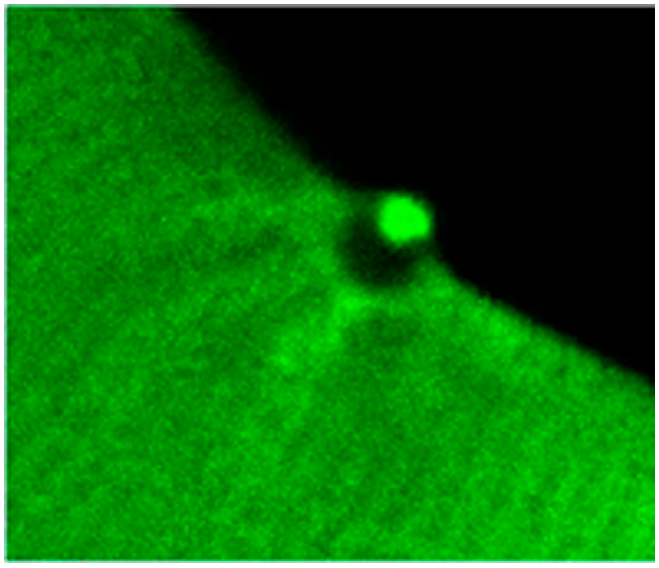

Movie S4. ANXA6-GFP orchestrates repair after laser induced sarcolemma disruption. The sarcolemma of myofibers expressing ANXA6-GFP was damaged using a laser. The background strain was 129 to avoid the effect of the severe *Anxa6* allele. A representative time lapse movie is shown. ANXA6-GFP forms a tight large cap over a clear repair zone. In FM4-64 imaging performed concurrently (Movie S5), this vesicle-rich nature of this repair zone is visualized.

Movie S4

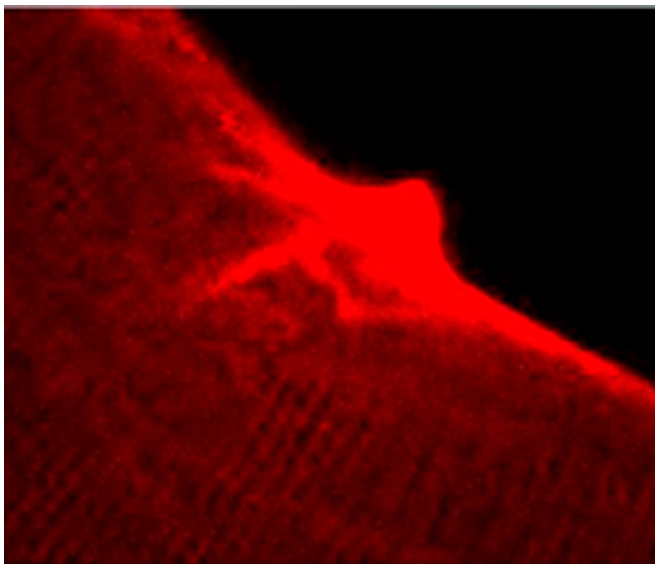

Movie S5. FM4-64 dye imaging of laser-injured myofiber expressing ANXA6-GFP. Laser-induced damage was used in the presence of FM4-64 to asses sarcolemmal injury and repair. A representative time lapse movie of the ANXA6-GFP expressing myofiber from Movie S4 is shown. FM4-64 binds to vesicles accumulating at the site of injury immediately under the ANXA6-GFP cap.

Movie S5

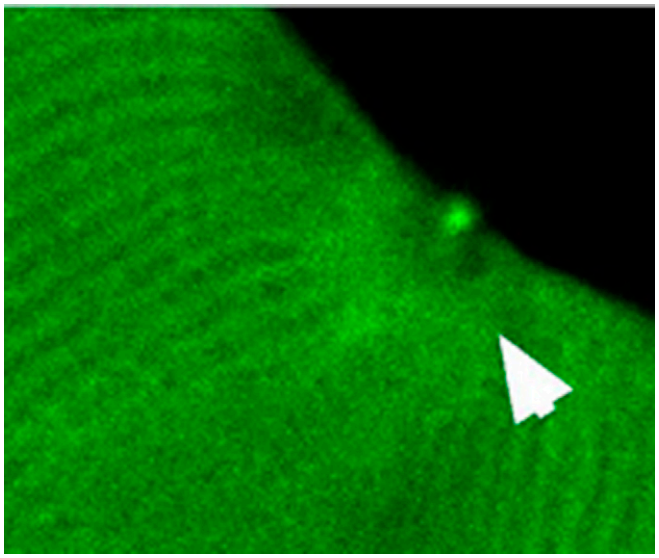

Movie S6. ANXA6N32 disrupts the cap and repair zone after sarcolemmal disruption. Myofibers expressing ANXA6N32-GFP were damaged using a laser. As in the previous experiment, myofibers from the 129 background were used. A representative time lapse movie of an ANXA6N32-GFP expressing fiber is shown. ANXA6N32-GFP forms a much smaller cap, and visual caps were seen in only 44% of the fibers expressing ANXA6N32-GFP, whereas they were present in 100% of fibers expressing ANXA6-GFP. Furthermore, the clear repair zone under the cap does not persist throughout the window of imaging (5 min). Compare results to Movie S4, where the cap remains visible for the entire window of imaging (5 min). This premature closure of the repair zone is associated with leak of contents (Movie S7).

Movie S6

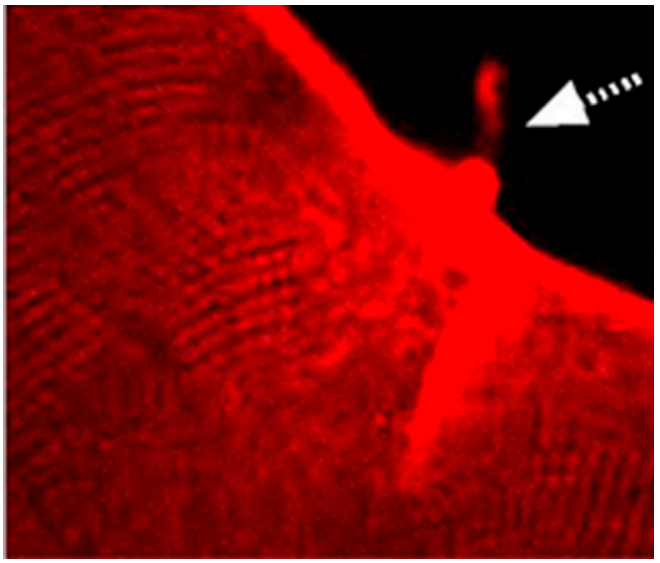

Movie S7. FM4-64 dye imaging of the laser injured ANXA6N32-GFP myofiber. A representative time lapse movie of an ANXA6N32-GFP of the laser-injured fiber from Movie S6 is shown. FM4-64 accumulates in vesicles under the site of injury, but in the presence of the weakened cap and disorganized repair zone, FM4-64 vesicles leak from the myofiber into the extracellular space.

Movie S7

Other Supporting Information Files

Table S1 (XLS)